

Synthesis of ZnO nanoparticles by hydrothermal method

P. M. Aneesh, K. A. Vanaja, M. K. Jayaraj*

Optoelectronic Devices Laboratory, Cochin University of Science and Technology, Kochi-682 022,
India

ABSTRACT

Stable, OH free zinc oxide (ZnO) nanoparticles were synthesized by hydrothermal method by varying the growth temperature and concentration of the precursors. The formation of ZnO nanoparticles were confirmed by x-ray diffraction (XRD), transmission electron microscopy (TEM) and selected area electron diffraction (SAED) studies. The average particle size have been found to be about 7-24 nm and the compositional analysis is done with inductively coupled plasma atomic emission spectroscopy (ICP-AES). Diffuse reflectance spectroscopy (DRS) results shows that the band gap of ZnO nanoparticles is blue shifted with decrease in particle size. Photoluminescence properties of ZnO nanoparticles at room temperature were studied and the green photoluminescent emission from ZnO nanoparticles can originate from the oxygen vacancy or ZnO interstitial related defects.

Key words: Hydrothermal, ZnO, band gap, particle size, photoluminescent emission

*Corresponding author
Tel: +91-484-2577404
Fax: +91-484-2577595
Email: mkj@cusat.ac.in

1. INTRODUCTION

Semiconductors with dimensions in the nanometer realm are important because their electrical, optical and chemical properties can be tuned by changing the size of particles. Optical properties and are of great interest for application in optoelectronics, photovoltaics and biological sensing. Various chemical synthetic methods have been developed to prepare such nanoparticles.

Zinc Oxide (ZnO) is a unique material with a direct band gap (3.37eV) and large exciton binding energy of 60meV^{1, 2}. It has been widely used in near-UV emission, gas sensors, transparent conductor and piezoelectric application³⁻⁷. Most of the ZnO crystals have been synthesized by traditional high temperature solid state method which is energy consuming and difficult to control the particle properties. ZnO¹¹⁻¹³ nanoparticles can be prepared on a large scale at low cost by simple solution - based methods, such as chemical precipitation^{8, 9}, sol-gel synthesis¹⁰, and solvothermal/hydrothermal reaction¹¹⁻¹³. Hydrothermal technique is a promising alternative synthetic method because of the low process temperature and very easy to control the particle size. The hydrothermal process have several advantage over other growth processes such as use of simple equipment, catalyst-free growth, low cost, large area uniform production, environmental friendliness and less hazardous. The low reaction temperatures make this method an attractive one for microelectronics and plastic electronics¹⁴. This method has also been successfully employed to prepare nano-scale ZnO and other luminescent materials. The particle properties such as morphology and size can be controlled via the hydrothermal process by adjusting the reaction temperature, time and concentration of precursors.

The present study focuses on the hydrothermal synthesis of ZnO nanopowders and the effect of reaction temperatures, concentration of the precursors and time of growth on its properties. The hydrothermal synthesis of ZnO powders has four advantages (1) powders with nanometer- size can be obtained by this method (2) the reaction is carried out under moderate conditions (3) powders with different morphologies by adjusting the reaction conditions and (4) the as-prepared powders have different properties from that of the bulk.

2. EXPERIMENTAL DETAILS

In order to synthesize the ZnO nanoparticles, stock solutions of Zn(CH₃COO)₂·2H₂O (0.1 M) was prepared in 50ml methanol under stirring. To this stock solution 25ml of NaOH (varying from 0.2 M to 0.5 M) solution prepared in methanol was added under continuous stirring in order to get the pH value of reactants between 8 and 11. These solutions was transferred into teflon lined sealed stainless steel autoclaves and maintained at various temperature in the range of 100 - 200°C for 6 and 12 h under autogenous pressure. It was then allowed to cool naturally to room temperature. After the reaction was complete, the resulting white solid products were washed with methanol, filtered and then dried in air in a laboratory oven at 60°C.

The synthesized samples were characterized for their structure by x-ray diffraction (Rigaku D max-C) with Cu K α radiation. Transmission electron microscopy (TEM) selected area electron diffraction (SAED) and high resolution transmission electron microscopy (HRTEM) were performed with a JEOL JEM-3100F transmission electron microscope operating at 200 kV. The sample for TEM was prepared by placing a drop of the ZnO suspension in methanol onto a standard carbon coated copper grid. The grids were dried before recording the micrographs. The optical band gap E_g was estimated from the UV-Vis-NIR diffuse reflectance spectroscopic (UV-Vis-NIR DRS) studies in a wavelength range from 190nm to 1200nm with JASCO V-570 spectrophotometer. The samples for this study were used in the form of powder and pure BaSO₄ used as the reference. The elemental composition of the ZnO nanoparticles were determined by using Thermo Electron IRIS INTREPID II XSP DUO inductively coupled plasma atomic emission spectrometer (ICP-AES). Room temperature photoluminescence (PL) of the samples was measured on Horiba Jobin Yuon Fluoromax-3 spectrofluorimeter using Xe arc lamp as the excitation source.

3. RESULTS AND DISCUSSION

The x-ray diffraction data were recorded by using Cu K α radiation (1.5406 Å). The intensity data were collected over a 2 θ range of 20-80°. The average grain size of the samples was estimated with the help of Scherrer equation using the diffraction intensity of (101) peak.

x-ray diffraction studies confirmed that the synthesized materials were ZnO with wurtzite phase and all the diffraction peaks agreed with the reported JCPDS data¹⁵ and no characteristic peaks were observed other than ZnO.

The mean grain size (D) of the particles was determined from the XRD line broadening measurement using Scherrer equation¹⁶.

$$D=0.89\lambda / (\beta\text{Cos}\theta)$$

Where λ is the wavelength (Cu K α), β is the full width at the half- maximum (FWHM) of the ZnO (101) line and θ is the diffraction angle.

A definite line broadening of the diffraction peaks is an indication that the synthesized materials are in nanometer range. The grain size was found to be in the range of 7-24 nm depending on the growth condition. The lattice parameters calculated were also in agreement with the reported values.

The reaction temperature greatly influences the particle morphology of as-prepared ZnO powders. Figure 1 shows that the XRD patterns of ZnO nanoparticles synthesized at various temperature with 0.3 M NaOH for 6 h. As the reaction temperature increases, FWHM decreases. Thus the size of ZnO nanoparticles increases as the temperature for the hydrothermal synthesis increases. This is due to the change of growth rate between the different crystallographic planes.

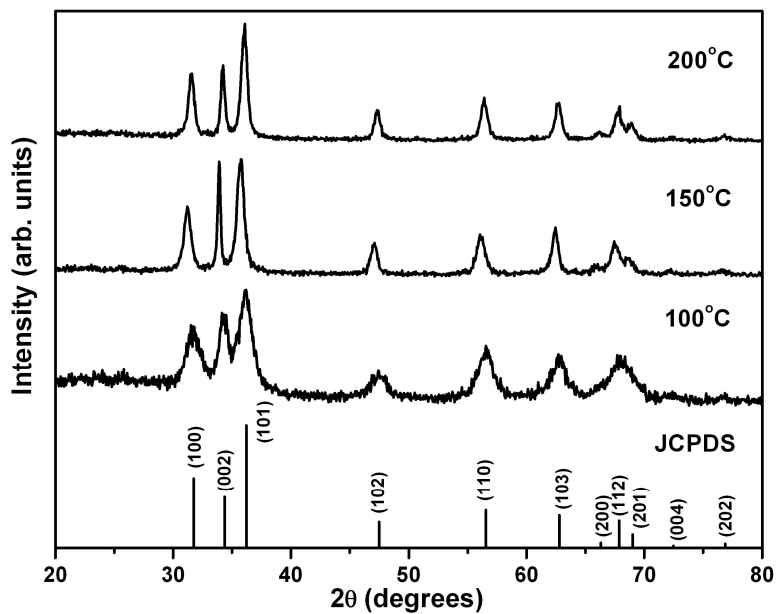


Fig. 1. XRD patterns of ZnO nanoparticles synthesized from 0.3 M NaOH at various temperatures for 6 h.

Figure 2 shows the variation of FWHM and grain size of ZnO nanoparticles synthesized from 0.3 M NaOH at different temperatures for a growth time of 6 h. The average grain size calculated by Scherrer equation is observed to increase from 7 nm to 16 nm as the temperature increases from 100°C to 200°C¹⁷.

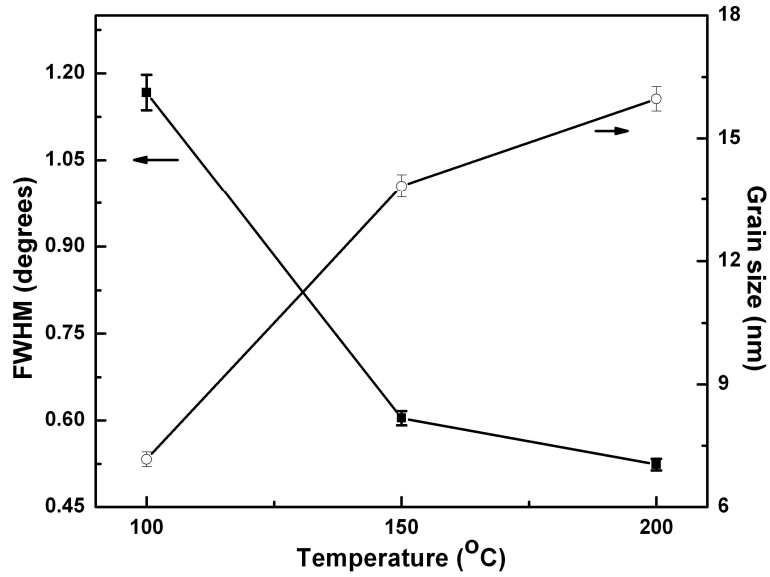


Fig. 2. Variation of FWHM and grain size of ZnO nano particles synthesized from 0.3 M NaOH with temperature for a growth time of 6 h.

ZnO structures with different grain sizes can be obtained by controlling the concentration of the precursors. ZnO nanoparticles were synthesized by keeping the concentration of $\text{Zn}(\text{CH}_3\text{COO})_2 \cdot 2\text{H}_2\text{O}$ as 0.1 M in all reactions, the concentration of NaOH was varied from 0.2 M to 0.5 M at 200°C for 12 h. Figure 3 shows the XRD pattern of ZnO nanoparticles synthesized by varying the concentration of precursors. All the peaks match well with the standard wurtzite structure¹⁵ and the FWHM of the (101) diffraction peak increases with the decreasing concentration of the NaOH. These results reveal that the molar ratio of OH^- to Zn^{2+} is a dominant factor for the formation of the ZnO nanoparticles.

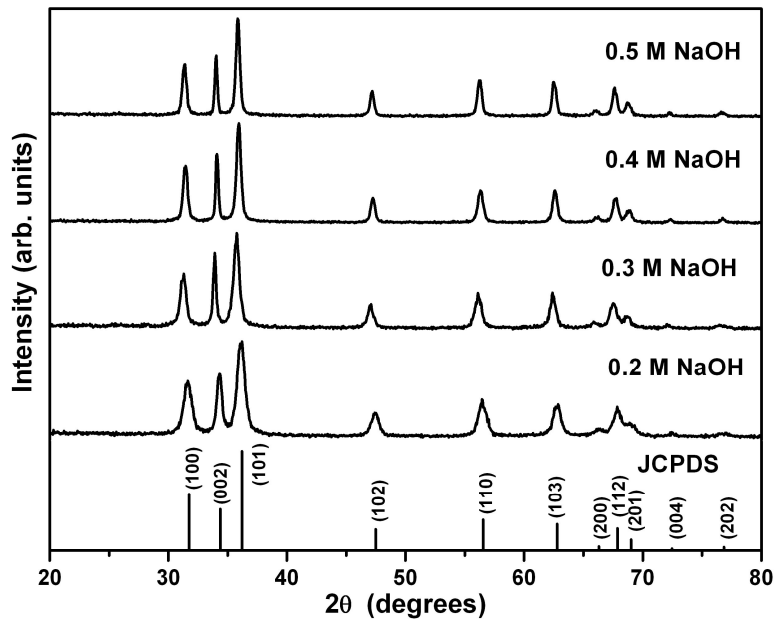


Fig. 3. XRD patterns of ZnO nanoparticles synthesized at various concentration of NaOH (0.2 M, 0.3 M, 0.4 M, and 0.5 M) at 200°C for 12 h.

Figure 4 shows the variation of FWHM and grain size of ZnO nanoparticles with concentration of NaOH precursor for the samples grown at 200°C for 12 h. It has a linear variation with the concentration of NaOH precursor. The grain size increases from 12 nm to 24 nm as the concentration of NaOH precursors increases from 0.2 M to 0.5 M.

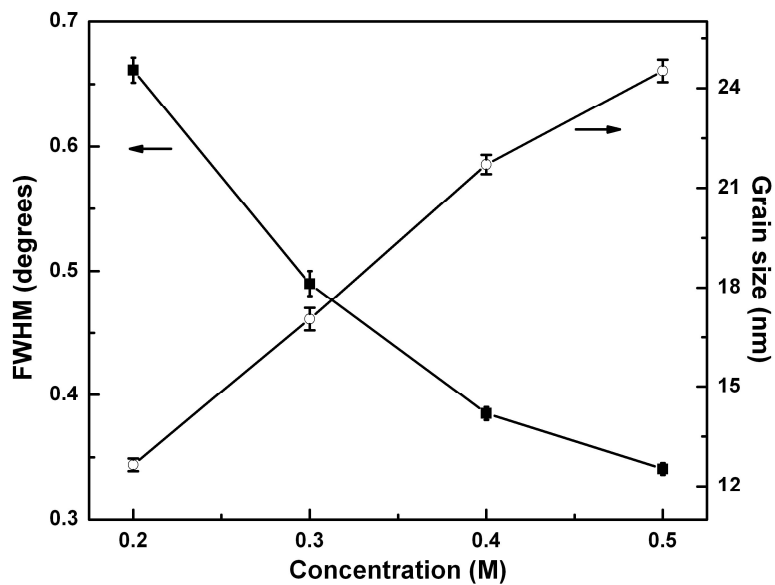


Fig. 4. Variation of FWHM and grain size of ZnO nano particle with various concentration of NaOH grown at 200°C for a growth time of 12 h.

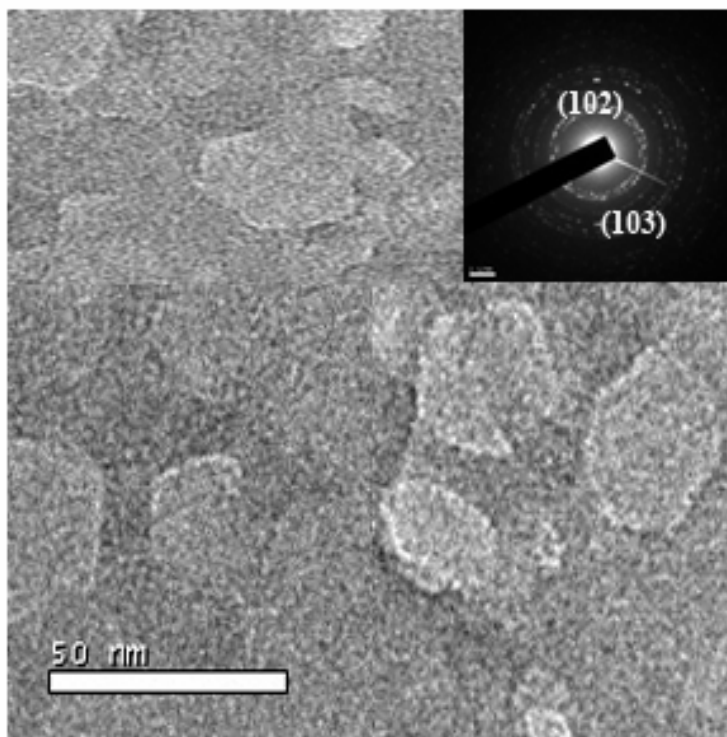
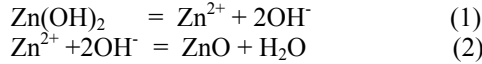


Fig. 5.) TEM image of the ZnO nanoparticles synthesized from 0.5 M NaOH at 150°C for 6 h . Inset shows the SAED image

In the precursor solution used in the experiment, the source of Zn is in the forms of Zn(OH)₂ precipitates and Zn(OH)₄²⁻ species according to the stoichiometric ratio of Zn²⁺ on OH⁻. The Zn(OH)₂ precipitates under the hydrothermal conditions will dissolve to considerable extent to form ions of Zn²⁺ and OH⁻, once the product of [Zn²⁺] and [OH⁻] exceeds a critical value which is necessary for the formation of ZnO crystals, the ZnO crystals will precipitate from the solution. The solubility of ZnO is significantly smaller than that of Zn(OH)₂ under the hydrothermal conditions, consequently, the Zn(OH)₂ precipitates strongly tended to be transformed into ZnO crystals during the hydrothermal process, by the following reactions^{18, 19}.



At the initial stage of the process, the concentrations of Zn²⁺ and OH⁻ were relatively higher so that the crystal growth in different directions was considerable^{18, 20}. When the concentration of Zn²⁺ and OH⁻ reaches the supersaturation degree of ZnO, ZnO begins to nucleate and the crystal growth begins.

Figure 5 shows the TEM image and corresponding selected-area electron diffraction (SAED) pattern of the ZnO nanoparticles synthesized at 150°C for 6 h from 0.5 M NaOH. TEM image confirms the formation of ZnO nanoparticle and it has an average size about 25 nm. From the diffraction rings of SAED pattern shown in the inset of figure 5, (102) and (103) planes of the ZnO nanoparticles were identified.

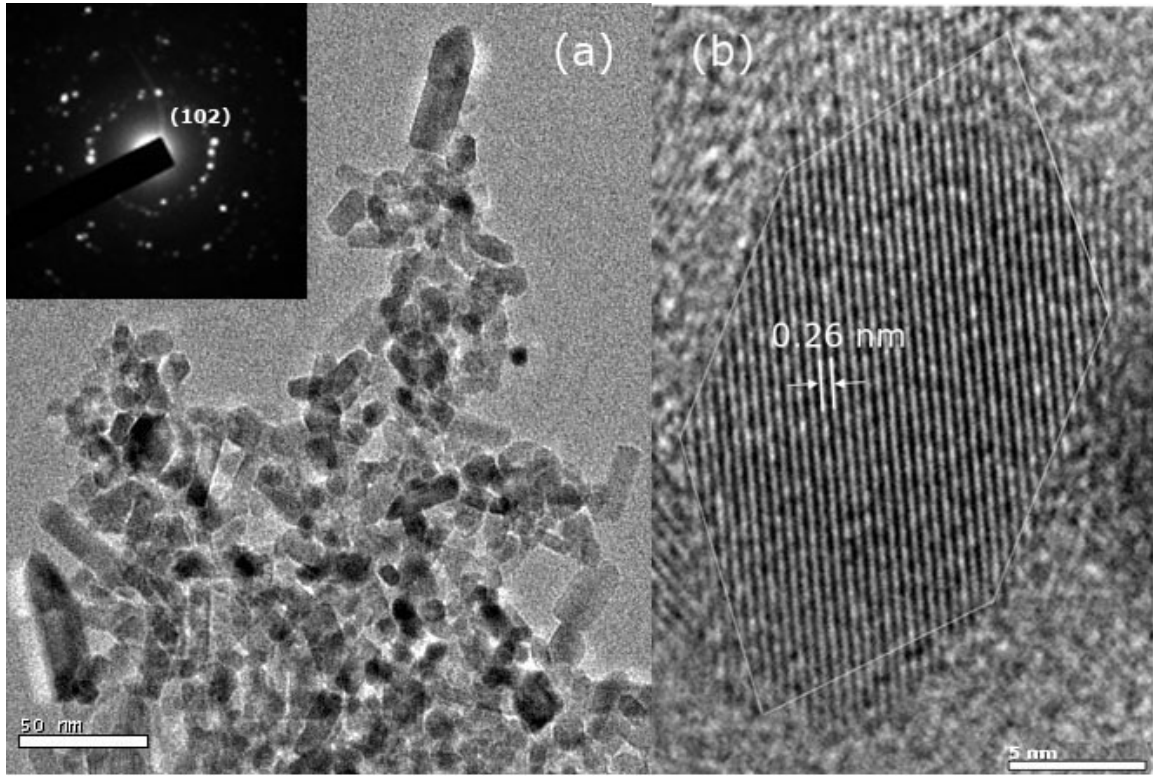


Fig.6. (a) TEM image of the ZnO nanoparticles synthesized from 0.3 M NaOH at 150°C for 6 h . Inset shows the SAED image (b) HRTEM of the ZnO nanoparticle.

Figure 6(a) shows the TEM image and corresponding selected-area electron diffraction (SAED) pattern of the ZnO nanoparticle synthesized at 150°C for 6 h from 0.3 M NaOH. TEM image confirms the formation of ZnO nanoparticle with an average size about 10 nm. Some ZnO nanorods with average diameter of 15nm and length of about 50nm were also observed. From the diffraction rings of SAED pattern shown in the inset of figure 6(a), (102) plane of the ZnO nanoparticles were identified. Figure 6(b) shows the HRTEM image of the ZnO nanoparticle synthesized at

150°C for 6 h from 0.3 M NaOH. HRTEM pattern indicates that the nanorods grow along the *c* axis and it has standard hexagonal structure.

Diffuse reflectance spectral studies in the UV- Vis- NIR region were carried out to estimate the optical band gap of the synthesized nanoparticles. Figure 7 shows the plot for the percentage of reflection as a function of band gap energy ($h\nu$) of the nanoparticles synthesized via hydrothermal method from 0.3 M NaOH at 100°C for 6 h. The band gap estimated for this sample 3.42eV that is slightly higher than that of bulk ZnO (3.37eV). This blue shift may be attributed to quantum confinement effects.

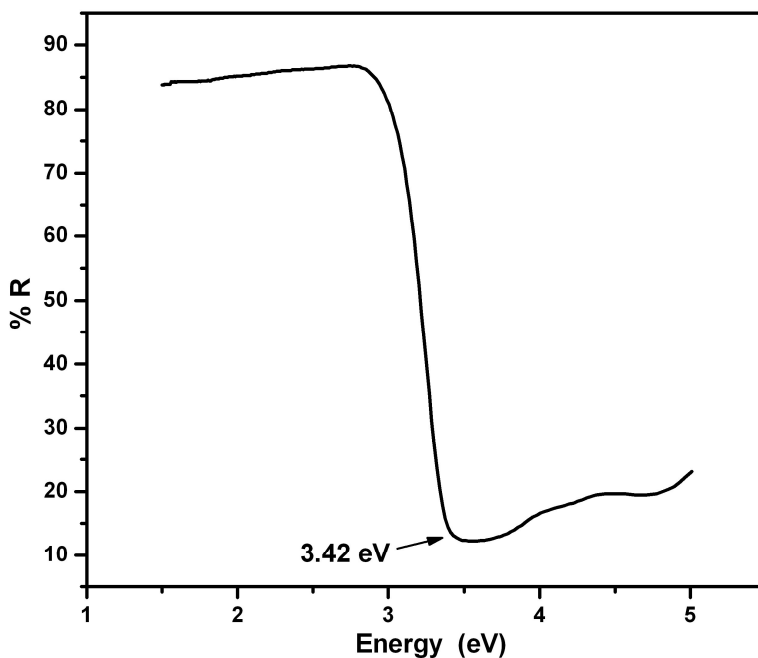


Fig. 7. DRS of the typical ZnO nanoparticles synthesized from 0.3 M NaOH at 100°C for 6 h

The amount of Na that is incorporated in ZnO nanoparticles was determined using ICP-AES data. The ICP-AES shows that Na incorporated into the nanoparticles is about 0.17% for lower concentration and about 1.49% for higher concentration of NaOH in the precursor solution. The Na content in the ZnO nanoparticles increases with NaOH concentration. The theoretical binding energy of dopant atoms on the individual semiconductor nanocrystal surface determines its doping efficiency²¹. The binding energy for wurtzite semiconductor nanocrystal is three times less than that of zinc blend or rock salt structure on (001) faces. The low concentration of incorporated Na is likely to be a consequence of lower doping efficiency of the wurtzite ZnO nanocrystal surfaces.

The luminescence of ZnO nanoparticles is one of particular interest from viewpoints of both physical and applied aspects. Figure 8 shows the room temperature photoluminescence spectrum of the ZnO nanoparticles excited at 362 nm.

Green emission was observed from the hydrothermally synthesized ZnO nanoparticles. It can be attributed to the transition between singly charged oxygen vacancy and photo excited hole or Zn interstitial related defects^{22, 23}. The inset in the figure 8 shows the photoluminescent excitation spectra of the ZnO nanoparticles ($\lambda_{em} = 545\text{nm}$) which indicates that the excitation is at 362 nm. The excitation peak corresponds to the band to band transition which also confirms the blue shift in the band gap of ZnO nanoparticles.

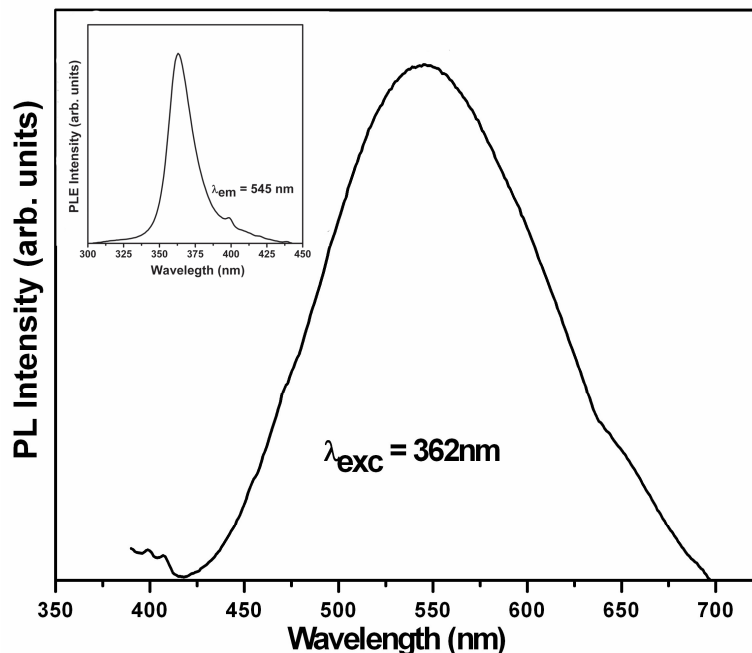


Fig. 8. Room temperature photoluminescence spectra of ZnO nanoparticle excited at $\lambda_{exc} = 362$ nm. The inset shows the corresponding photoluminescent excitation spectra ($\lambda_{em} = 545$ nm) of ZnO nanoparticles.

4. CONCLUSIONS

ZnO nanoparticles were synthesized using hydrothermal method. The effect of concentration of the precursors, temperature and time of growth on the structure, grain size, band gap energy, and PL were investigated. The XRD analysis demonstrates that the nanoparticles have the hexagonal wurtzite structure and the particle size increases with growth temperature and decreases with concentration of the precursors. Due to quantum confinement effects, the band gap of the ZnO nanoparticles is blue shifted compared with the bulk material. The green PL emissions observed for the synthesized ZnO nanoparticles is due to the oxygen vacancy or Zn interstitial defects.

5. ACKNOWLEDGMENT

The work is supported by Department. of science and technology, Government of India under Nanoscience and Technology Initiative. One of the author (PMA) thanks Kerala State Council for Science, Technology and Environment for the award of research fellowship and SPIE for the travel support.

6. REFERENCES

- 1) Gyu-Chul Y, Chunrui W. and Won Il P. "ZnO nanorods: synthesis, characterization and applications" *Semicond. Sci. Technol.* **20**, S22, 2005
- 2) Qiuxiang Z, Ke Y, Wei B, Qingyan W, Feng X, Ziqiang Z, Ning D, Yan S, "Synthesis, optical and field emission properties of three different ZnO nanostructures", *Materials Letters*, **61**, 3890, 2007
- 3) Yuzhen L, Lin G, Huibin X, Lu D, Chunlei Y, Jiannong W, Weikun G, and Shihe Y, Ziyu W, "Low temperature synthesis and optical properties of small-diameter ZnO nanorods", *J. Appl. Phys.* **99**, 114302, 2006
- 4) Hachigo A, Nakahata H, Higaki K, Fujii S and Shikata S-I, "Heteroepitaxial growth of ZnO films on diamond (111) plane by magnetron sputtering", *Appl. Phys. Lett.* **65**, 2556, 1994
- 5) Morkoc H, Strite S, Gao G B, Lin M E, and Sverdlov B, and M. Burns, "Large-band-gap SIC, III-V nitride, and II-VI ZnSe-based semiconductor device technologies", *J. Appl. Phys.* **76**, 1363, 1994

- 6) Spanhel L and Anderson M A, "Semiconductor Clusters in the Sol-Gel Process: Quantized Aggregation, Gelation, and Crystal Growth in Concentrated ZnO Colloids", *J. Am. Chem. Soc.*, **113**, 2826, 1991
- 7) Bagnall D M, Chen Y F, Shen M Y, Zhu Z, Goto T and Yao T, "Room temperature excitonic stimulated emission from zinc oxide epilayers grown by plasma-assisted MBE", *J. Cryst. Growth*, **184/185**, 605, 1998
- 8) Zhong Q P and Matijevic E, "Preparation of uniform zinc oxide colloids by controlled double-jet precipitation", *J. Mater. Chem.*, **3**, 443, 1996
- 9) Lingna W and Mamoun M, "Synthesis of zinc oxide nanoparticles with controlled morphology", *J. Mater. Chem.*, **9**, 2871, 1999
- 10) Bahnmann D W, Kormann C and Hoffmann M R "Preparation and Characterization of Quantum Size Zinc Oxide: A Detailed Spectroscopic Study", *J. Phys. Chem* **91**, 3789, 1987
- 11) Hui Z, Deren Y, Xiangyang M, Yujie J, Jin X and Duanlin Q, "Synthesis of flower-like ZnO nanostructures by an organic-free hydrothermal process" *Nanotechnology* **15**, 622, 2004
- 12) Zhang J, Sun L D, Yin J L, Su H L, Liao C S and Yan C H, "Control of ZnO Morphology via a Simple Solution Route", *Chem. Mater.*, **14**, 4172, 2002
- 13) Li W J, Shi E W, Zheng Y Q and Yin Z W, "Hydrothermal preparation of nanometer ZnO powders", *J. Mater. Sci. Lett.*, **20**, 1381, 2001
- 14) Lee. C.Y, Tseng T. Y, Li. S. y, Lin.P, "Effect of phosphorus dopant on photoluminescence and field-emission characteristics of $Mg_{0.1}Zn_{0.9}O$ nanowires", *J. Appl. Phys.*, **99**, 024303, 2006
- 15) JCPDS Card No. 36-1451
- 16) Klug H P and Alexander L E. *X-ray diffraction Procedures for polycrystalline and Amorphous Materials*, 1st edn, chapter 9, Wiley, New York, 1954
- 17) Zhijian W, Haiming Z, Ligong Z, Jinshan Y, Shenggang Y and Chunyan W, "Low-temperature synthesis of ZnO nanoparticles by solid-state pyrolytic reaction", *Nanotechnology*, **14**, 11, 2003
- 18) Ahsanulhaq Q, Umar A and Hahn Y B, "Growth of aligned ZnO nanorods and nanopencils on ZnO/Si in aqueous solution: growth mechanism and structural and optical properties", *Nanotechnology* **18**, 115603, 2007
- 19) Xiangyang M, Hui Z, Yujie J, Jin X, Deren Y, "Sequential occurrence of ZnO nanoparticles, nanorods, and nanotips during hydrothermal process in a dilute aqueous solution", *Materials Letters*, **59**, 3393, 2005
- 20) Tok. A.I.Y, Boey. F.Y.C, Du. S.W and Wong. B.K, "Flame spray synthesis of ZrO_2 nano-particles using liquid precursors", *Materials Science and Engineering: B* **130**, 114, 2006
- 21) Steven C.E, Lijun Z, Michael I.H, Alexander L. E, Thomas A. K & David J. N, "Doping semiconductor nanocrystals", *Nature*, **436**, 91, 2005
- 22) Vanheusden K, Warren W L, Seager CH, Tallant DR, Voigt J A, Gnade B. E, *J Appl Phys* **79**, 7983, 1996
- 23) Peng. W.Q, Qu. S.C, Cong. G.W, Wang. Z.G, "Structure and visible luminescence of ZnO nanoparticles", *Materials Science in Semiconductor Processing*, **9**, 156, 2006